



ORIGINAL ARTICLE

HOXD8 suppresses renal cell carcinoma growth by upregulating SHMT1 expression

Yang Yang^{1,2}  | Minghui Zhang^{1,2} | Yaxuan Zhao^{1,2} | Tingzhi Deng^{1,2} | Xiang Zhou^{1,2} | Hanxu Qian^{1,2} | Mengxuan Wang^{1,2} | Chuanchuan Zhang^{1,2} | Zhengjin Huo³ | Zijun Mao³ | Zhufeng Shao¹ | Mengxue Liu¹ | Chunhua Yang^{1,2} | Chunhua Lin⁴  | Fuyi Xu^{1,2} | Geng Tian^{1,2} | Yin Zhang^{1,2}

¹School of Pharmacy, Binzhou Medical University, Yantai, China

²Shandong Technology Innovation Center of Molecular Targeting and Intelligent Diagnosis, and Treatment, Binzhou Medical University, Yantai, China

³The First School of Clinical Medicine, Binzhou Medical University, Yantai, China

⁴Department of Urology, The Affiliated Yantai Yuhuangding Hospital of Qingdao University, Yantai, China

Correspondence

Yin Zhang and Geng Tian, School of Pharmacology, Binzhou Medical University, 346 Guanhai Road, Yantai, Shandong 264003, China.

Email: yin_zhang@bzmc.edu.cn and tiangeng@bzmc.edu.cn

Funding information

Major Basic Research Project of Shandong Provincial Natural Science Foundation, Grant/Award Number: ZR2019ZD27; National Natural Science Foundation of China, Grant/Award Number: 82103391; Natural Science Foundation of Shandong Province for Excellent Youth Scholars, Grant/Award Number: ZR2021MH292; Special Project of Central Government for Local Science and Technology Development of Shandong Province, Grant/Award Number: YDZX20203700001291; Taishan Scholar's program, Grant/Award Number: tsqn201812100; Youth Science Foundation project of Shandong Province Natural Science Foundation, Grant/Award Number: ZR2020QH242; Taishan Scholars Construction Engineering to GT, Grant/Award Number: tstp20221145

Abstract

Amplification of amino acids synthesis is reported to promote tumorigenesis. The serine/glycine biosynthesis pathway is a reversible conversion of serine and glycine catalyzed by cytoplasmic serine hydroxymethyltransferase (SHMT)1 and mitochondrial SHMT2; however, the role of SHMT1 in renal cell carcinoma (RCC) is still unclear. We found that low SHMT1 expression is correlated with poor survival of RCC patients. The in vitro study showed that overexpression of SHMT1 suppressed RCC proliferation and migration. In the mouse tumor model, SHMT1 significantly retarded RCC tumor growth. Furthermore, by gene network analysis, we found several SHMT1-related genes, among which homeobox D8 (HOXD8) was identified as the SHMT1 regulator. Knockdown of HOXD8 decreased SHMT1 expression, resulting in faster RCC growth, and rescued the SHMT1 overexpression-induced cell migration defects. Additionally, ChIP assay found the binding site of HOXD8 to SHMT1 promoter was at the -456~-254 bp region. Taken together, SHMT1 functions as a tumor suppressor in RCC. The transcription factor HOXD8 can promote SHMT1 expression and suppress RCC cell proliferation and migration, which provides new mechanisms of SHMT1 in RCC tumor growth and might be used as a potential therapeutic target candidate for clinical treatment.

KEYWORDS

BXD, HOXD8, RCC, serine/glycine synthesis, SHMT

Abbreviations: ccRCC, clear cell renal cell carcinoma; CDC20, cycle protein 20; GWAS, genome-wide association study; HOXD8, homeobox D8; RCC, renal cell carcinoma; ROS, reactive oxygen species; SHMT, serine hydroxymethyltransferase; SSP, serine synthesis pathway; THF, tetrahydrofolate; TSS, transcription start site.

Yang Yang, Minghui Zhang, and Yaxuan Zhao contributed equally to this work.

This is an open access article under the terms of the [Creative Commons Attribution-NonCommercial-NoDerivs](https://creativecommons.org/licenses/by-nc-nd/4.0/) License, which permits use and distribution in any medium, provided the original work is properly cited, the use is non-commercial and no modifications or adaptations are made.

© 2023 The Authors. *Cancer Science* published by John Wiley & Sons Australia, Ltd on behalf of Japanese Cancer Association.

1 | INTRODUCTION

Renal cell carcinoma (RCC) is a malignant tumor originating from the renal tubular epithelial cells. RCC accounts for about 2%–3% of adult malignant tumors and 80%–90% of adult renal malignant tumors, and its incidence has increased rapidly worldwide in the past few decades.¹ Although great achievements have been made in the diagnosis and treatment of RCC, the 5-year survival rate of patients with metastatic RCC is only 12% due to the high risk of metastasis and poor response to current therapies.^{2–4} This highlights the necessity to develop novel therapeutic targets for RCC.

One-carbon metabolism provides substrates for nucleotide synthesis and DNA methylation which is linked to cancer progression. Blocking one carbon unit utilization has been used as a therapeutic target for several chemotherapeutic drugs (methotrexate and pemetrexed) by inhibiting thymidine synthase that utilizes 5,10-methylene tetrahydrofolate (THF) (5,10-Methylenetetrahydrofolate).⁵ Several studies found an association between the one-carbon metabolism pathway genes' polymorphisms and RCC risk.^{6–8} The serine/glycine synthesis pathway (SSP) is the main source of one-carbon units in cancer cells. Interestingly, some tumors are highly dependent on serine uptake to support cancer cell proliferation, in which increased dietary serine promoted faster tumor growth in animal models.^{9,10} Additionally, other studies have suggested the activation of the SSP as an adaptation for survival after radiation exposure.¹¹ These data suggest a major contribution of the SSP in tumor growth. Nevertheless, no existing intervention strategies specifically target the SSP in cancer therapy. Therefore, further investigation is required into the mechanisms that induce SSP hyperactivation in cancer, which may contribute to the development of anticancer drugs.

Serine hydroxymethyltransferase (SHMT) is the central enzyme of the SSP. SHMT catalyzes the reversible conversion of serine and THF to glycine and 5,10-methylene THF. There are two isoforms of SHMT, which are cytoplasmic SHMT1 and mitochondrial SHMT2.¹² Accumulating evidence confirmed that SHMT2 facilitates cell proliferation and tumor growth,¹³ and SHMT2 overexpression is tightly associated with poor prognosis in various cancers.^{14–18} Also, SHMT1 has recently been found to play critical roles in cancers. SHMT1 upregulated the expression of the oncogenic procytokines interleukin-6/-8 and promoted the growth and migration of ovarian cancer cells.¹⁹ In lung cancer, knockout of SHMT1 led to cell cycle arrest and p53-dependent apoptosis by increasing uracil accumulation during DNA replication.²⁰ In addition, the expression level of SHMT1 was inversely correlated with clinical prognostic factors in breast cancer.²¹ These studies suggested that SHMT1 acts as oncoprotein and promotes the progression of these cancers. However, Dou et al. found that SHMT1 inhibited the ability of liver cancer cells to metastasize, and SHMT1 knockdown enhanced the production of reactive oxygen species (ROS).²² In summary, both the two SHMT isoenzymes and serine metabolism play an important role in the progression of different tumors. Studies have shown that high expression of SHMT2 facilitated RCC cell proliferation by inducing the G1/S phase transition and predicted poor overall survival in RCC

patients.²³ However, the expression and function of cytoplasmic SHMT1 in RCC remain uncovered.

In this study, we found that low-expression SHMT1 in RCC tissues was associated with pathological grading and poor prognosis of RCC patients. Overexpression of SHMT1 effectively led to G2/M cell cycle arrest and inhibited the proliferation and migration of RCC cells. In addition, we explored the regulation factor of SHMT1 expression and function in RCC cells through genome-wide association studies. Further study showed that the transcription factor HOXD8 regulated SHMT1 expression and suppressed RCC cell proliferation and migration. In summary, our findings reveal that cytoplasmic SHMT1 regulated by HOXD8 suppresses the proliferation and migration of RCC cells.

2 | MATERIALS AND METHODS

2.1 | GEPIA data analysis

The GEPIA2 online analysis tool (<http://gepia2.cancer-pku.cn/#analysis>) was used to analyze the expression and correlation of the overall survival rate of SHMT1 in kidney renal clear cell carcinoma (KIRC) patients. The clinical significance and the correlation with SHMT1 of GRB14, SP5, HOXD8, and HOXD9 in KIRC were analyzed using GEPIA2.

2.2 | Cell culture and transfection

Human RCC cell lines OSRC-2 and ACHN were purchased from Procell Life Science & Technology (CL-0177, CL-0021). OSRC-2 and ACHN cells were cultured in RPMI-1640 or Minimum Essential Medium, respectively, supplemented with 10% fetal bovine serum, 50U/mL penicillin, and 0.1mg/mL streptomycin. All cells were maintained at 37°C in 5% CO₂.

The pcDNA3.1-Flag-SHMT1 (NM_148918) and pcDNA3.1-Flag-HOXD8 (NM_019558.4) plasmids were purchased from Vigene Biosciences. pGL4.11-SHMT1(Human)-Promoter-fLuc-hPEST plasmid was purchased from Miaoling bio (P33783). The siRNA against HOXD8 and SHMT1 were obtained from GeneChem. The siRNA sequences used were as follows: 5'-GCCGAAGGCCUGACAAA UUAATT-3', 5'-CUGACGGAGCUGGCUACAAATT-3'. The control siRNA sequences used were as follows: sense strand: UUCUCCGA ACGUGACACGUdTdT; nonsense strand: ACGUGACACGUUCG GAGAAAdTdT. Cells were transfected by JetPRIME (Polyplus) according to the manufacturer's protocol. Cells were harvested at 48–72h post transfection for future experiments.

2.3 | Cell viability assay

Cell Counting Kit-8 (CCK-8) (B34304, Bimake) was used to perform the cell viability assay. A total of 2000 cells were seeded per well

in 96-well culture plates. After the cell was attached to the wall, CCK8 was added at 10% concentration to each well and incubated at 37°C for 1 h. The absorbance of cells was determined at 450 nm by BioTek Epoch every 24 h for 4–5 days. For the MTHFD2 inhibition experiment, cells were treated with DS18561882 (HY-130251, MCE) for 5 days at the concentration of 15 μM or transfected with siHOXD8 before harvesting cells for sample preparation.

2.4 | Cell migration assays

Twenty-four-well plates containing 8-mm pore size transwell chambers (3244#, Corning, USA) were used to assess tumor cell migration; 5×10^4 cells in serum-free medium were seeded into the upper chamber for the migration experiment. A complete medium was added to each lower chamber. The cells were incubated for 24 or 48 h at 37°C. Cells that migrated through the pores were fixed with methanol for 10 min and stained with 0.1% crystal violet after incubation. Cell count and photograph were taken using an IX71 inverted microscope (Olympus).

2.5 | Scratch assay

Confluent cell dish was scratched with a sterile 200 μL plastic tip and then continued to culture for 48 h. The scratched gaps were photographed by the microscope. Cell relative gaps were measured by image J software.

2.6 | RNA extraction and RT-qPCR

Total RNA was isolated from cells using Trizol (15596026#, Invitrogen). Reverse transcription of total RNA to cDNA was performed using the reverse transcriptase (R323-010, Vazyme). RT-qPCR was performed using SYBR qPCR Mix (Q711-02, Vazyme). Primer sequences used were as follows: SHMT1-F: 5'-CTGGCACAACCCCTCAAAGA-3'; SHMT1-R: 5'-AGGCAATCAGCTCCAATCCA-3'; HOXD8-F: 5'-GGAAGACAAACCTACAGTCGC-3'; HOXD8-R: 5'-TCCTGGTCAGATAGGGGTTAAAA-3'; Actin-F: ACCTTCTACAATGAGCTGCGT, Actin-R: TAGCAACGTACATGGCTGGG. Relative quantitation of gene expression was calculated using the $2^{-\Delta\Delta CT}$ method.

2.7 | Western blot

Total proteins were extracted using cell lysis buffer (P0013, Beyotime) and separated by SDS-PAGE. Then, proteins were transferred onto polyvinylidene fluoride (PVDF) membranes (Millipore). After blocking with 5% skim milk, the membranes were incubated with primary antibodies against SHMT1 (1:1000, D3B3J, CST), cyclinB (1:1000, 4138S, CST), CDC20 (1:1000, 4823S, CST), β-actin (1:1000, A00702, GenScript), HOXD8 (1:1000, sc-515357, SantaCruz), p21 (1:1000, A1483, ABclonal), γ-H2AX (1:500, CSB-PA010097OA139phHU,

CUSABIO), p-CDK1 (1:1000, CSB-PA000492, CUSABIO), p-CHK1 (1:1000, CSB-PA006769, CUSABIO), p-CDC25 (1:1000, CSB-PA080107, CUSABIO), cyclinE (1:1000, sc-377100, SANTA), and cyclinD (1:1000, WL01435a, WanleiBio) overnight at 4°C with shaking. Then, the membranes were washed with Tris Buffered Saline with Tween20 (TBST) and incubated with secondary antibody conjugated with HRP (1:5000, GenScript) for 1 h at room temperature. The signals were developed by the ECL detection kit (Wanleibio).

2.8 | Xenograft tumor experiment

BALB/c nude mice aged 6–8 weeks were purchased from Gempharmatech Co., Ltd. OSRC-2 cells expressing SHMT1, or empty vector were prepared into single cell suspension. Then, 1×10^7 cells were subcutaneously injected into the back of each mouse. Tumor volume was measured every 2 days and calculated with the formula: tumor volume (mm^3) = $(\text{length} \times \text{width}^2)/2$. Mice were sacrificed when the tumor volume reached a size of 1000 mm^3 . Tumors were fixed with 4% paraformaldehyde and embedded to make paraffin sections, following by immunohistochemical (IHC) staining.

2.9 | Immunohistochemical staining assay

Tumor tissue sections from 13 patients with RCC were obtained from Yantai Yuhuangding Hospital. All individuals who donated tissues for this study provided written consent. The IHC staining assay was performed in accordance with the manufacturer's instructions (GK600510, Gene Tech). The primary antibodies were used against SHMT1 (1:200, 80715#, CST), Ki67 (1:200, 9449#, CST), CC3 (1:100, 9661L, CST), p21 (1:100, 10355-1-AP, Proteintech), and p-CDK1-T161 (1:100, CSB-PA000492, CUSABIO). Two histopathologists were blindly assigned to review the slides and score the staining. Staining of tissue sections were scored according to the following standards: staining intensity was classified as 0 (lack of staining), 1 (mild staining), 2 (moderate staining), or 3 (strong staining); the percentage of staining was designated 1 (<25%), 2 (25%–50%), 3 (51%–75%), or 4 (>75%). For each section, the semiquantitative score was calculated by multiplying these two values (which ranged from 0 to 12).²⁴

2.10 | Luciferase reporter assay

Luciferase reporter assay was used to detect the activity of the SHMT1 promoter. HEK293T cells were seeded in 24-well plates at a density of 2.0×10^5 cells per well. When growing to the confluence at 40%–50%, the cells were transfected with siRNA against HOXD8 by using JetPRIME transfection reagent, and then the cells were cotransfected with plasmids pGL4.11-SHMT1(Human)-Promoter-fLuc and pcDNA3.1-Flag-HOXD8 or pcDNA3.1 by using the JetPRIME transfection reagent after 24 h of siHOXD8 transfection. Luciferase activity was examined with a Luciferase Reporter Assays Substrate Kit (RG005, Beyotime) by

a microplate reader. β -gal activity of each transfected well was used to normalize the luciferase activity.

2.11 | Chromatin immunoprecipitation (ChIP) assay

ChIP assay was performed using a ChIP Kit (9003#, Cell Signaling Technology). OSRC-2 cells (4×10^6 cells per sample) were cross-linked by 1% formaldehyde and sonicated by 5-s pulses/10-s intervals for 5 min. The digested chromatin samples were then immunoprecipitated with HOXD8 antibody or IgG antibody (negative control) and enriched by magnetic beads. After elution and purification, the immunoprecipitated DNA samples were analyzed by qPCR with the following primers for ChIP: SHMT1-P1-F: GTGCTGCTCTTGGATTATACACCT; SHMT1-P1-R: CTTTGTAGTTGTCAGGGTGGTCA; SHMT1-P2-F: TTTATGACGCGCCTCAGGT; SHMT1-P2-R: ACTGACACACAATAAGGACTCA.

2.12 | BXD mice kidney gene expression data

This data set was accessed on the GeneNetwork website (www.genenetwork.org). The BXD mice kidney gene expression data were obtained through the "Mouse Kidney M430v2 (Jul06) Robust Multi-array Average (RMA)" dataset, which provides estimates of mRNA expression in the adult kidney of 56 genetically diverse strains of mice including 53 BXD recombinant inbred strains, one F1 hybrid (D2B6F1), and two parental strains (B6 and D2). Kidney samples were processed using a total of 153 Affymetrix Mouse Expression 430 2.0 microarrays (M430v2.0). This data set was processed using the RMA protocol.

2.13 | Expression quantitative trait locus (eQTL) mapping

The eQTL mapping of *Shmt1* expression variation in BXD mice kidney was conducted using a WebQTL module in GeneNetwork according to published methods.^{25,26} Likelihood ratio statistics (LRS) were calculated and used to measure the association or linkage between differences in traits and differences in specific genotype markers. eQTL significance was evaluated using 2000 permutation tests. The eQTL confidence interval was estimated by 1.5 LOD (limit of detection) drop-off interval. eQTL genes were then crossed to the genes correlated with the *Shmt1* expression to screen the candidate genes.

2.14 | Construction of mutant HOXD8 and SHMT1 promoter

ATTA on the P1 region of plasmid pGL4.11-SHMT1(Human)-PromoterLuc was mutated into CGTA directly with a site-directed mutagenesis

kit (11003ES10, Yeasen). The HOXD8 plasmid was linearized by using restriction endonuclease NheI and XhoI. Two segments besides HOXD8 DNA binding segments in HOXD8 were amplified separately by PCR and purified by Gel Extraction Kit (Omega Bio-Tek) after electrophoresis in agarose gel. These two DNA fragments were cloned to linearized vector through the KpnI and SmaI clone sites with the Hieff Clone One Step Cloning Kit (10911ES08, Yeasen). HOXD8 mutant plasmid, which knocked out the DNA binding region (197–256 amino acids), was constructed. Luciferase assays were performed in 293T cells with the pGL4.11-SHMT1 promoter-mutated luciferase reporter and HOXD8 mutant plasmid described above. Primers were as follows: SHMT1- Δ P1-F: TGCTCTTGGGcTATACCTACAGAGTAATAATGTTGCAGTT, SHMT1- Δ P1-R: GTGTATAgcCCAAGAGCAGACACTTTATTATTATTATT.

2.15 | Single-cell gel electrophoresis (alkaline comet assay)

An alkaline comet assay was performed by using the ELK Comet assay kit (CA001, ELK Biotechnology) according to the manufacturer's protocol. Olive tail moment (OTM) as a product of the tail length and the percentage of total DNA in the tail was applied to evaluate DNA damage. Comet images were captured with the Axio Imager M2 fluorescent microscope (Carl Zeiss).

2.16 | Statistical analysis

Data were presented in the form of mean \pm standard deviation (SD), and each experiment was independently repeated more than three times. Statistical analyses were performed using Graphpad Prism 5 (GraphPad Software Inc). Data were analyzed for statistical significance by Student's *t*-test or one-way analysis of variance (ANOVA). $p < 0.05$ was considered statistically significant.

3 | RESULTS

3.1 | Low expression of SHMT1 correlates with poor survival of RCC patients

To explore the clinical significance of SHMT1 in RCC, we analyzed the relative expression of SHMT1 in RCC patients (KIRC) in different stages using the GEPIA 2 online analysis tool. The results showed that SHMT1 expression was decreased with the stages progressed in KIRC patients (Figure 1A). Moreover, compared with high-SHMT1-level patients, the overall survival rate was significantly lower in low-SHMT1-level patients (Figure 1B). Further, RCC patient samples showed that SHMT1 was lower in RCC tissues than adjacent tissues (Figure 1C,D). Staining of SHMT1 in tumor tissues from 13 patients with RCC also demonstrated lower expression of SHMT1 in RCC tissues (Figure 1E,F). Taken together, these results

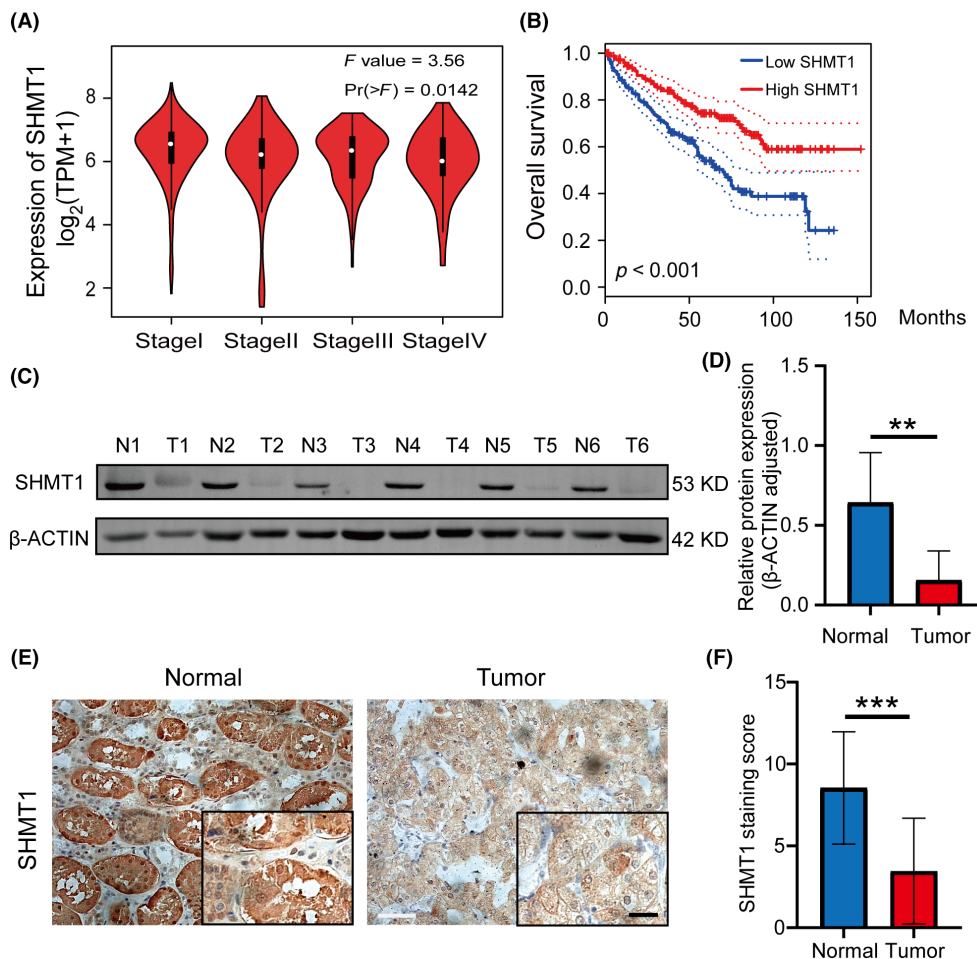


FIGURE 1 Serine hydroxymethyltransferase (SHMT)1 expression in renal cell carcinoma (RCC) tissues and correlations to survival. (A) Expression of SHMT1 in RCC patients (KIRC) in different stages analyzed with the GEPIA2 online tool. $n=258$ patients. (B) Kaplan-Meier analysis was performed to evaluate the association between SHMT1 level and RCC patients' overall survival by GEPIA2. (C, D) Detection of SHMT1 expression by Western blot in RCC tissues and adjacent tissues from six RCC patients. $n=6$ samples. (E, F) Representative immunohistochemistry staining of SHMT1 protein level in RCC tumor tissues and adjacent tissues from 13 RCC patients. $n=13$ pair of samples. White color scale bars: 100 μ m, black color scale bars: 50 μ m. ** $p < 0.01$, *** $p < 0.001$.

suggest that the expression of SHMT1 is reduced in human RCC tissues and correlated with the progression and poor prognosis of RCC patients.

3.2 | SHMT1 inhibits RCC cell proliferation and metastasis in vitro

To further investigate the role of SHMT1 in RCC cells, we established stable overexpressing SHMT1 (OE-SHMT1) cell lines, OSRC-2 and ACHN. Western blot analysis verified that SHMT1 was significantly overexpressed in OE-SHMT1 cells (Figure 2A). CCK8 assay showed that OE-SHMT1 inhibited the proliferation of RCC cells (Figure 2B). To explore how SHMT1 inhibited proliferation of RCC cells, flow cytometry was performed to detect the effect of SHMT1 on the cell cycle, which showed that SHMT1 induced G2/M phase arrest in OSRC-2 (Figure S1A,B). To investigate the underlying mechanisms, we tested multiple cell cycle-related proteins in

SHMT1-overexpression RCC cells. The G2/M check points-related proteins such as p-CDC25, p-CDK1, and cyclin B/D/E were decreased,²⁷ suggesting SHMT1-induced cell cycle arrest was due to the conventional signaling pathway. Interestingly, cell division cycle protein 20 (CDC20) was also decreased, which suggested a defect of chromosome segregation during mitotic exit (Figure S1C).²⁸ As DNA damage is one of the causes of cell cycle arrest,²⁹ we checked the DNA damage marker p-CHK1 and γ -H2AX. Consistent with the cell cycle proteins, these two markers were increased in SHMT1-overexpression RCC cells (Figure S1C). Further, we performed a single-cell gel electrophoresis, which further demonstrated the DNA damage by the nuclei tail length (Figure S1D). In addition, both cell scratch assay and transwell assay showed that overexpressing SHMT1 efficiently reduced the migration of OSRC-2 and ACHN cells (Figure 2C,D). On the contrary, SHMT1 knockdown in OSRC-2 and ACHN cells showed increased cell migration and cell proliferation (Figure 2E-G). These results illustrated that SHMT1 has a potential inhibitory role in regulating RCC cell progression.

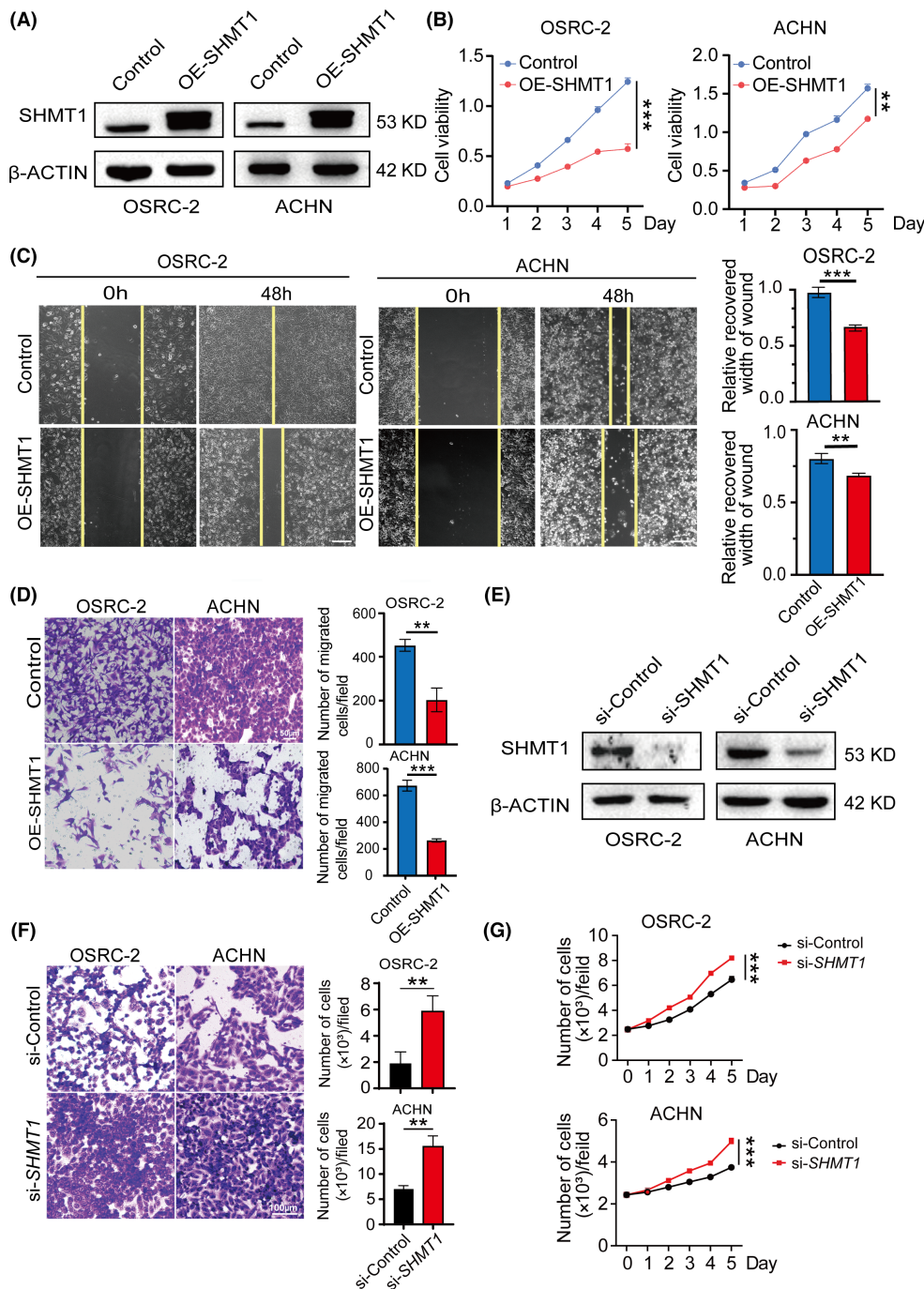


FIGURE 2 Serine hydroxymethyltransferase (SHMT)1 inhibits cell proliferation and migration in renal cell carcinoma (RCC) cells. (A) SHMT1 expression in OSRC-2 and ACHN cells transfected with pcDNA3.1-Flag-SHMT1(OE-SHMT1) and vector plasmid (Vector). (B) Cell proliferation assay by CCK8 assay in OSRC-2 and ACHN cell lines. (C) Scratch assay of SHMT1-overexpressed OSRC-2 and ACHN cells. Scale bars: 100 μ m. (D) Transwell assay of SHMT1-overexpressed OSRC-2 and ACHN cells. Scale bars: 50 μ m. (E) Western blot validation of SHMT1 expression by siRNA transfection. (F) Transwell assay of SHMT1 knockdown OSRC-2 and ACHN cells. Scale bars: 100 μ m. (G) Cell proliferation of SHMT1 knockdown OSRC-2 and ACHN cells. $n=3$ samples; all experiments were repeated twice. ** $p < 0.01$, *** $p < 0.001$.

3.3 | SHMT1 suppresses RCC cell growth in vivo

To confirm the biological function of SHMT1 on RCC growth in vivo, a xenograft tumor model was established by subcutaneously injecting control or OE-SHMT1-OSRC-2 cells into nude mice. Compared with the control group, the OE-SHMT1 group significantly

inhibited tumor growth (Figure 3A,B), and the tumor weight of the OE-SHMT1 group was significantly reduced (Figure 3C). The staining of cell proliferation marker Ki67 also showed a sharp decrease along with the increase of SHMT1 staining in tumor tissues (Figure 3D). In addition, the apoptotic marker cleaved caspase 3 staining also increased in the SHMT1-overexpressed tumor tissues. Together

with the increase of p21 and decrease of phosphorylated CDK1, these data demonstrated the inhibition of tumor proliferation and apoptosis by SHMT1 (Figure 3E). Collectively, these data demonstrate that SHMT1 suppresses the growth of RCC cell in vivo.

3.4 | Shmt1 expression is transregulated by Hoxd8 in BXD mice kidney

To identify the regulators of SHMT1 in RCC, we performed an analysis by genome-wide association studies (GWAS). As a high-energy resource of GWAS, the BXD family is widely used in the study of medicine and disease mechanism, including the search for

the regulatory network of genes in diseases.^{30,31} Figure 4A shows the gene expression levels of Shmt1 in kidney tissue from 53 BXD mouse strains and their corresponding parental strains. To identify the genetic loci that regulate the expression of Shmt1 in kidney, we performed simple interval mapping for Shmt1 across the mouse genome. A significant expression QTL (eQTL) was identified on chromosome (Chr) 2 at 65–75 Mb (Figure 4B). This locus was distantly located from the genomic location of Shmt1 (Ch11 at 60.78 Mb), suggesting that Shmt1 was transregulated.

To find out the potential factors that regulate Shmt1, we took the 160 genes in the 1.5 LOD QTL interval and intersected by the top 2000 genes that correlated with Shmt1 by Pearson correlation coefficient (Figure 4C). We found eight candidates (Cobl1,

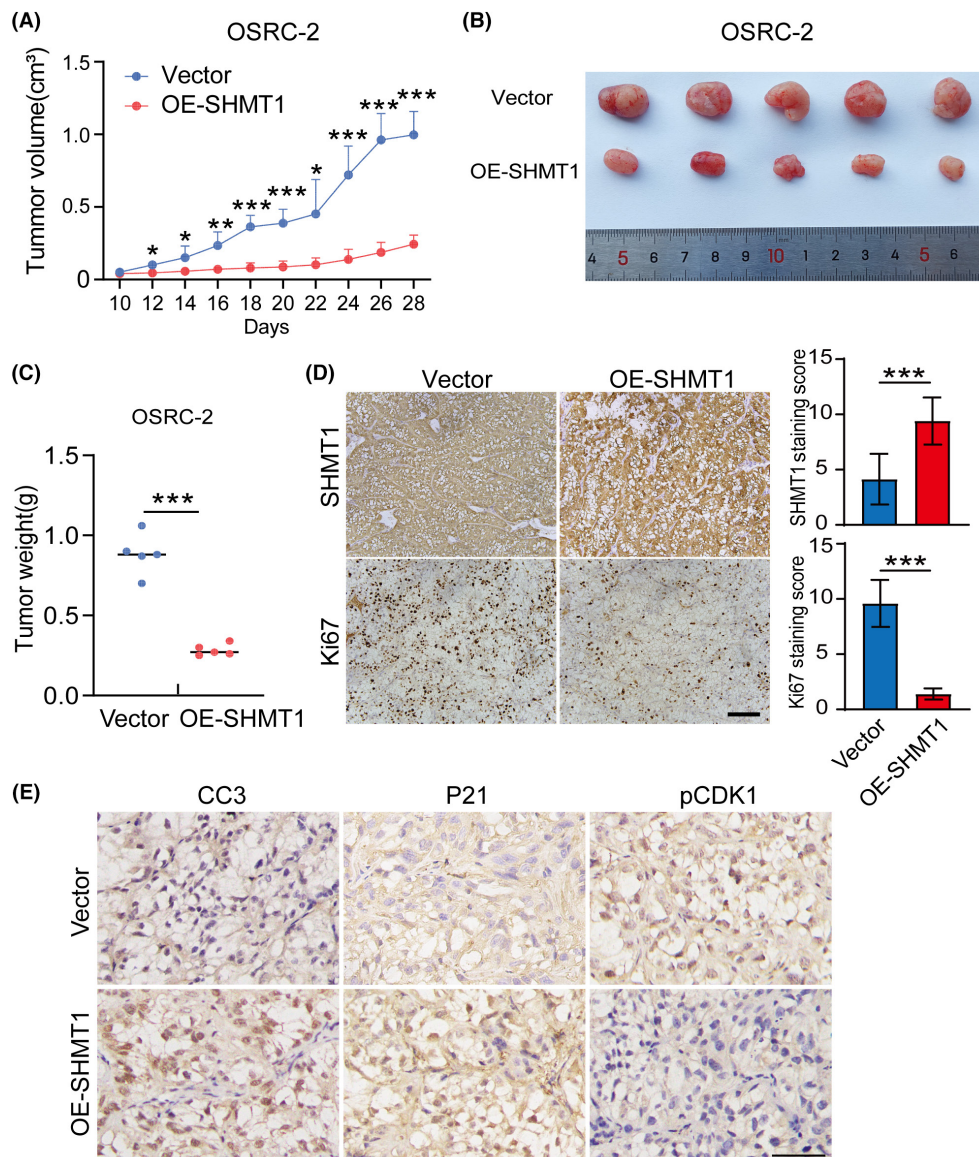


FIGURE 3 Serine hydroxymethyltransferase (SHMT)1 inhibits OSRC-2 tumor growth in vivo. (A) Tumor volume and tumor weight of tumor in vector ($n=5$) and SHMT1-overexpression tumor ($n=5$). (B) The captured image of tumors shows the tumor size of two groups. (C) Tumor weight of tumor in vector ($n=5$) and SHMT1-overexpression tumor ($n=5$). (D) Immunohistochemistry of SHMT1 and Ki67 and quantification. Scale bar: 100 μm . (E) Immunohistochemistry of cleaved caspase 3 (CC3), P21, and phosphorylated CDK1. Scale bar: 50 μm . * $p < 0.05$, ** $p < 0.01$, *** $p < 0.001$.

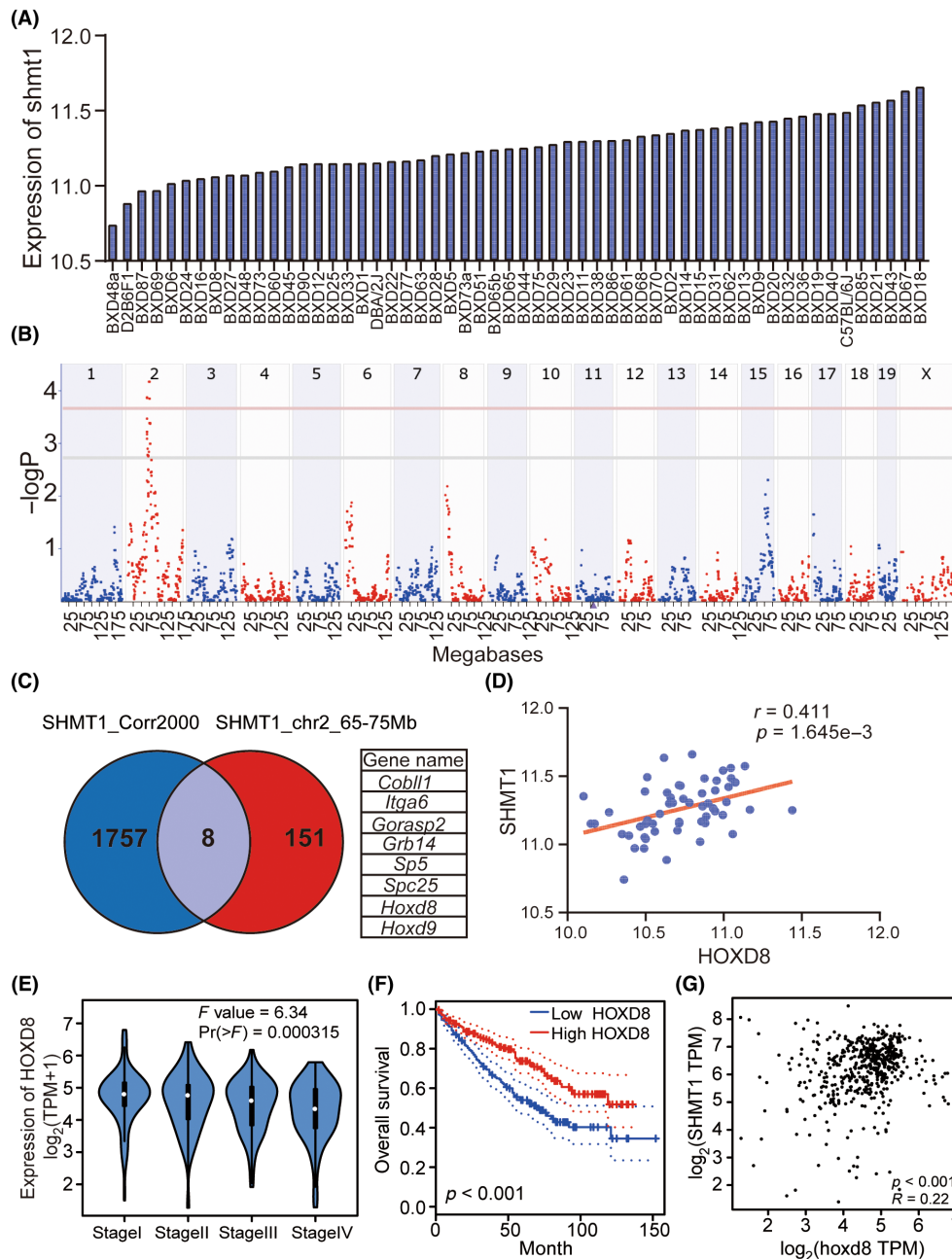


FIGURE 4 BXD family analysis of the upstream genes of serine hydroxymethyltransferase (*Shmt1*). (A) Bar plots of the *SHMT1* expression across the BXD kidney. The x-axis shows the BXD strains and F1 strains (D2B6F1) and two parental strains. The y-axis indicates the normalized \log_2 expression levels of *Shmt1*. (B) eQTL mapping of the *Shmt1* gene in BXD strains kidney. The upper x-axis shows the chromosome, the lower x-axis shows the location in megabases (Mb), and the y-axis indicates the $-\log(p)$ score, which shows the linkage between gene expression and genomic region. Gray and red horizontal lines indicate the significant and suggestive threshold of the $-\log(p)$ scores for eQTL mapping, respectively. (C) The top 2000 genes correlated with *Shmt1* were crossed with genes included in the 1.5 LOD QTL interval. (D) Correlation between *Shmt1* and *Hoxd8* in a BXD mice family. *Shmt1* has a positive correlation with *Hoxd8* among 53 BXD strains. The Pearson correlation r - and p -values are shown. (E) Expression of *HOXD8* in KIRC in different stages using the GEPIA2 website. (F) Kaplan-Meier analysis was performed to evaluate the association between *HOXD8* level and KIRC patients' overall survival using the GEPIA2 website. $n = 258$ patients. (G) Correlation between *SHMT1* and *HOXD8* in KIRC patients' database. *SHMT1* has a positive correlation with *HOXD8* ($r = 0.22$, $p < 0.001$).

Itga6, *Gorasp2*, *Grb14*, *Sp5*, *Spc25*, *Hoxd8*, and *Hoxd9* (Figure 4C), where *Grb14*, *Sp5*, *Hoxd8*, and *Hoxd9* are transcription factors, which may regulate *Shmt1* expression. Analysis from BXD mice databases showed that *Shmt1* expression is correlated with *Hoxd8*

expression, suggesting that *Hoxd8* may be a potential regulator of *Shmt1* (Figure 4D). Next, we analyzed the correlation of *GRB14*, *SP5*, *HOXD8*, and *HOXD9* with *SHMT1* (Figure 4E–G, Figure S2A–I). It was indicated that only *HOXD8* was linked to progression and poor

prognosis of KIRC patients and positively correlated with the expression of SHMT1 in KIRC (Figure 4E–G). Further analysis revealed that HOXD8 methylation correlated with low SHMT1 expression (Figure S2J). Based on these results, we speculate that HOXD8 may act as a tumor suppressor in RCC to regulate the function of SHMT1.

3.5 | Knockdown of HOXD8 restored the inhibitory effect of SHMT1 on RCC cells

To verify whether HOXD8 is a regulator of SHMT1 in RCC cells, we transiently transferred Flag-HOXD8 plasmid into OSRC-2 or ACHN cells respectively. Immunoblotting analysis confirmed that overexpression of HOXD8 upregulated SHMT1 (Figure 5A). On the contrary, knocked down HOXD8 reduced SHMT1 protein level in OSRC-2 and ACHN cells (Figure 5B). As GRB14 showed a weak correlation between GRB14 and SHMT1 in KIRC ($r = -0.18$, $p = 2.3 \times 10^{-5}$), we examined the role of GRB14 in regulating SHMT1 expression in Figure S2H. Although *Shmt1* and *Grb14* were positively correlated in the BXD mice kidney, GRB14 overexpression had no significant effect on the expression of SHMT1 in both OSRC-2 and ACHN cells (Figure S3A,B). So, we excluded the possibility of GRB14 in regulating SHMT1 in RCC. Further CCK8 assays demonstrated that knockdown of HOXD8 restored the cell proliferation inhibited by SHMT1 on RCC cells (Figure 5C). Meanwhile, the scratch assay showed that knockdown of HOXD8 partially restored the suppressed migration of OE-SHMT1 OSRC-2 and ACHN cells (Figure 5D). Further, HOXD8 knockdown in both OSRC-2 and ACHN cells resulted in recovered cell migration in the transwell analysis (Figure 5E). Ducker et al. reported that SHMT1 plays an essential role supporting tumor growth in the background of MTHFD2 knockout.³² Thus, suppression of SHMT1 may enhance the cell inhibition effect by MTHFD2 inhibition. To further validate if HOXD8 regulated RCC cell growth through SHMT1, we treated HOXD8-knockdown ACHN cells with the MTHFD2 inhibitor DS18561882. The results demonstrated that HOXD8 knockdown exhibited synthetic lethality by MTHFD2 inhibition (Figure S4A). To further investigate the role of the HOXD8-SHMT1 axis in RCC cells, we performed a single-cell gel electrophoresis assay to detect the DNA damage level induced by SHMT1 overexpression. Interestingly, OE-SHMT1 induced a large DNA tail from the nuclei, but not in the HOXD8-knockdown group, and siHOXD8 could rescue the DNA damage level in the OE-SHMT1 group. These results further validated that HOXD8-induced SHMT1 overexpression might cause DNA damage, leading to cell death (Figure S4B). Again, we tested DNA the damage markers p-CHK1 and γ -H2AX by Western blot, which showed significant increase in OE-SHMT1 cells, but decrease in siHOXD8 cells. Similarly, the G2/M phase-related proteins were downregulated by OE-SHMT1 but restored by siHOXD8 in OE-SHMT1 cells, demonstrating the role of the HOXD8-SHMT1 axis in regulating cell cycle signaling (Figure S4C). Taken together, these results suggested that HOXD8 regulated the proliferation and migration of RCC cells through elevating SHMT1 expression.

3.6 | HOXD8 acts as a transcription activator of SHMT1 in RCC cells

Since HOXD8 is a transcription factor, it may play a role in the regulation of *SHMT1* expression. First, we established a HOXD8-overexpressed cell line. RT-qPCR confirmed that the *SHMT1* mRNA expression level was dramatically increased in OSRC-2 cells transfected with pcDNA3.1-Flag-HOXD8 (Figure S5A), suggesting that *SHMT1* might be regulated by HOXD8. Therefore, we conducted a luciferase reporter assay with HEK293T cells to verify this hypothesis. The results exhibited that the luciferase activity in cells cotransfected with pcDNA3.1-Flag-HOXD8 increased 1.5-fold compared with the vector group (si-control group). To exclude the impact of endogenous HOXD8, we first knocked down the endogenous HOXD8 by siHOXD8 and then repeated the luciferase assay and found a more robust elevation of luciferase activity (Figure 6A). Similar results were observed in OSRC-2 and ACHN cells (Figure S5B,C). These data indicated HOXD8 can induce *SHMT1* promoter activity.

To identify the binding sequence of HOXD8 to *SHMT1* promoter, we performed a binding analysis using the JASPAR online tool and predicted four recognizing sequences with the core sequence ATTA of HOXD8 (Figure 6B). By analyzing *SHMT1* promoter, we found four motifs with the core sequence ATTA recognized by HOXD8 within 1000bp upstream of the transcription start site (TSS) of *SHMT1* (Figure S6A). Two primers were designed to amplify the -456~-254 region and -920~-521 region for the ChIP assay (Figure 6C). The ChIP assay identified that the *SHMT1* promoter at the -456~-254 region of the upstream TSS was more likely to be enriched by HOXD8 in OSRC-2 cells (Figure 6D), suggesting that HOXD8 was more likely to bind this region. To further validate this finding, we established a HOXD8-mutated plasmid, as well as an *SHMT1* promoter P1 region-mutated plasmid. Interestingly, either mutation resulted in defects on luciferase transcription in both 293T and ACHN cells by luciferase assay (Figure S6B,C). These data suggested that HOXD8 is a transcription activator of SHMT1 in RCC cells.

4 | DISCUSSION

Serine metabolism plays a role as the metabolic integrator of nutritional state in the process of cell physiology.^{33–35} The reversible interconversion of serine and glycine is catalyzed by either the cytosolic SHMT1 or mitochondrial SHMT2. Importantly, this reaction donates carbon units to the one-carbon metabolism network, required for the synthesis of protein, lipids, nucleic acids, and methylation reactions.^{36,37} In recent years, the activation of the SSP due to gene amplification and alterations of upstream regulators that promote key enzyme overexpression is considered to be involved in the occurrence of cancer, including RCC.^{5,9,10} Thus, it is imperative to know if SHMT1 is involved in activation of SSP.

Here, we found that SHMT1 has low expression in human RCC tissues and is linked to poor prognosis in RCC patients. Overexpressed SHMT1 inhibited the proliferation of RCC cells both in

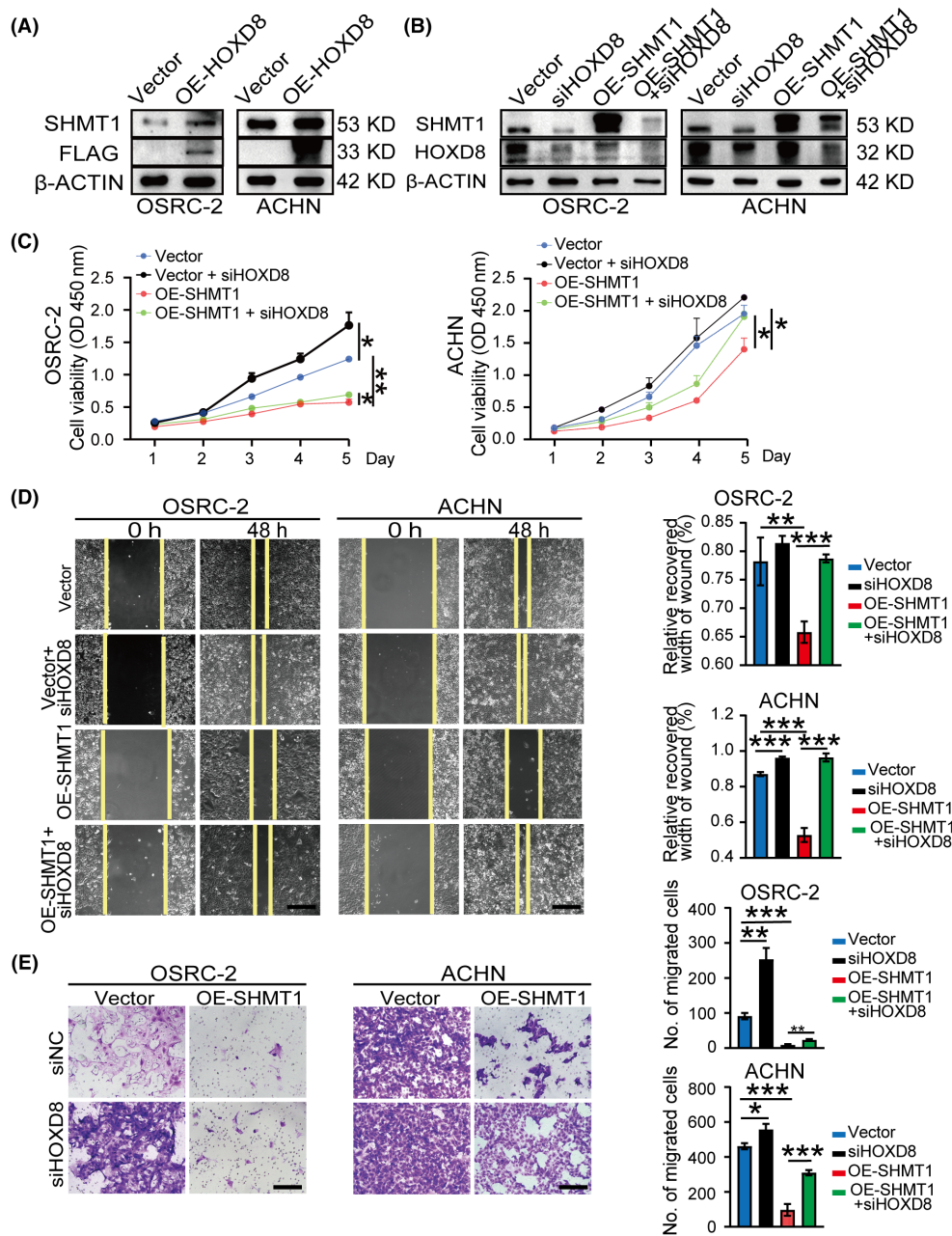


FIGURE 5 Knockdown of HOXD8 restores the inhibitory effect of serine hydroxymethyltransferase (SHMT)1 on renal cell carcinoma (RCC) cells. (A) The expression of SHMT1 and HOXD8 in OSRC-2 and ACHN cell transfected with pcDNA3.1-Flag-HOXD8 (OE-HOXD8) and vector plasmid (Vector). (B) Validation of SHMT1 expression in HOXD8-knockdown OSRC-2 and ACHN cells. (C) CCK8 assay showed the cell viability of OE-SHMT1 and control RCC cells transfected with siHOXD8 or siControl. (D) Scratch assay showed the migration ability of OE-SHMT1 and control RCC cells transfected with siHOXD8 or siControl. (E) Transwell assays were performed to verify the rescue role of knockdown HOXD8 in OE-SHMT1 RCC cells. C–E, $n = 3$ samples; all experiments were repeated twice. Scale: 100 μm . * $p < 0.05$, ** $p < 0.01$, *** $p < 0.001$.

vitro and in vivo, as well as migration in vitro. The results suggested that SHMT1 may act as tumor suppressor in RCC. Recently, Monti et al. discovered the SHMT2 mRNA-mediated crosstalk between SHMT isozymes in lung cancer cells, using this pattern to reprogram metabolism to get higher levels of available serine.^{23,38} We have considered that there may be a selective activation between SHMT isozymes to regulate compartmentalized serine metabolism in tumor cells. Therefore, it is more important for us to

further identify the dependent patterns of serine metabolism in tumor cells.

In addition to exploring the role of SHMT1 in RCC, we have also identified the upstream regulators of SHMT1 for understanding how SHMT1 function is misregulated in tumorigenesis. In our study, upstream regulatory genes of SHMT1 were analyzed using kidney transcriptome data of BXD family strains, a GWAS analytical model, in conjunction with the GEPIA2 tumor database. HOXD8 was identified

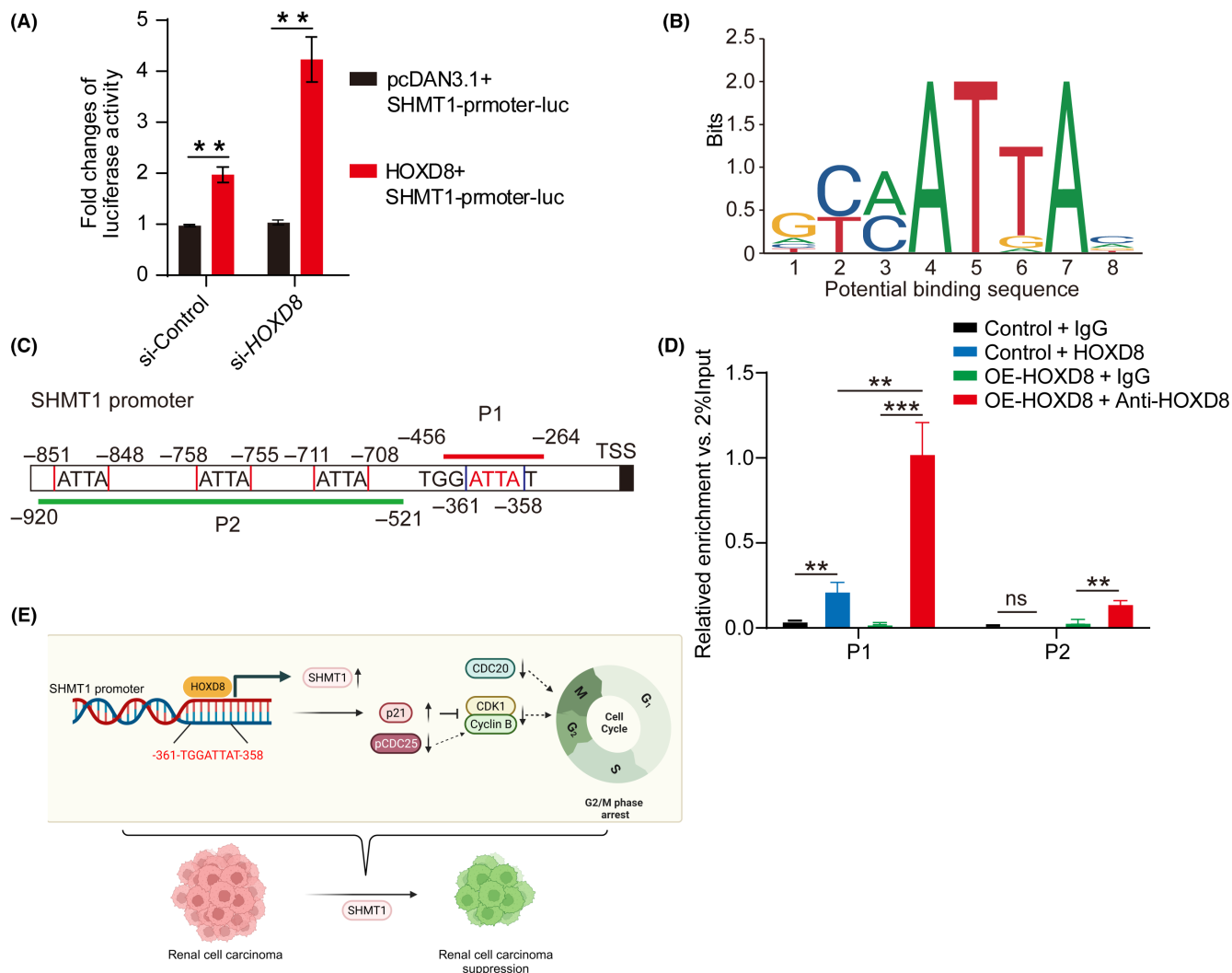


FIGURE 6 HOXD8 serves as a transcription activator of serine hydroxymethyltransferase (SHMT)1. (A) Luciferase reporter assay showed that HOXD8 targeted the SHMT1 gene promoter. 293T cells were transfected with siHOXD8 to knock down the endogenous HOXD8 first, followed by SHMT1-promoter-luc and pcDNA3.1-HOXD8 transfection. $n=3$ samples. (B) The prediction of binding motif and position of HOXD8 on SHMT1 promoter by JASPAR online analysis (<http://jaspar.genereg.net/>). (C) SHMT1 promoter analysis of potential binding region to HOXD8. P1 and P2 indicate the designed PCR product. TSS, transcription starting site. (D) ChIP-qPCR assays were performed to verify the HOXD8 binding regions in SHMT1 promoter. $n=3$ samples. $**p < 0.01$, $***p < 0.001$. (E) The illustration of HOXD8-induced renal cell carcinoma (RCC) inhibition. The transcription factor HOXD8 binds to the TGGATTAT sequence on SHMT1 promoter and upregulates SHMT1 expression. High level of SHMT1 results in cell cycle arrest through blocking multiple G2/M phase check points, such as p21, pCDC25, CDC20, as well as the CDK1/Cyclin B complex, leading to proliferation defects and finally tumor suppression.

as a regulator of SHMT1 in RCC and linked to tumor progression and poor prognosis of KIRC patients. More intriguingly, knockdown of HOXD8 restored the inhibitory effect of SHMT1 on RCC cells, and ChIP assay confirmed that HOXD8 acted as a transcription factor to activate SHMT1 in RCC cells. However, studies have shown that high expression of SHMT1 promotes ovarian cancer by inducing pro-oncogenic cytokines, such as IL-6/IL-8, through sialic acid stimulation.¹⁹ In lung cancer, SHMT1 knockdown induced P53 dependent apoptosis.²⁰ These findings implied that SHMT1 plays a cancer type-dependent role, and the expression level of SHMT1 has impacts on one-carbon unit metabolism but also involves a signaling pathway. Thus, the outcome of SHMT1 expression on tumor development depends on the specific tumor environment.

Worthy of note, overexpressed SHMT1 intensely led to G2/M phase cell cycle arrest in OSRC-2 cells and downregulated the expression of CDC20. CDC20 acts as an oncogenic role in a variety of human cancers including pancreatic cancer, breast cancer, and other cancers.³⁹⁻⁴¹ Studies strongly argue for CDC20 as a novel anticancer therapeutic drug target. Taniguchi et al. showed that depletion of CDC20 induced G2/M cell cycle arrest in pancreatic cells.⁴² We hypothesized that SHMT1 blocked chromosome separation and mitotic exit during the G2/M phase by downregulating CDC20. Additionally, other key check points were also inhibited by SHMT1 overexpression. The decreased activity of pCDC25 and the CDK1/Cyclin B complex and increased P21 altogether enhanced cell cycle arrest in G2/M phase. Altogether, these inhibitions on multiple

essential proteins led to RCC suppression (Figure 6E). However, the detailed mechanism needs to be further investigated.

In summary, our current findings demonstrate that SHMT1 functions as a tumor suppressor in RCC, which can be activated by the transcription factor HOXD8 (Figure 6E), presenting a novel therapeutic strategy focusing on the regulation of SSP enzymes for RCC. However, the complex dynamic structure of the SHMT active site has so far hindered the development of effective inhibitors,⁴³ and further elucidation of the mechanisms and clinical investigations are needed.

AUTHOR CONTRIBUTIONS

Yang Yang: Data curation; writing – original draft. **Minghui Zhang:** Conceptualization; writing – review and editing. **Yaxuan Zhao:** Investigation; writing – review and editing. **Tingzhi Deng:** Formal analysis. **Xiang Zhou:** Investigation. **Hanxu Qian:** Investigation. **Mengxuan Wang:** Investigation. **Chuanchuan Zhang:** Investigation. **Zhengjin Huo:** Investigation. **Zijun Mao:** Investigation. **Zhufeng Shao:** Investigation. **Mengxue Liu:** Investigation. **Chunhua Yang:** Resources. **chunhua lin:** Resources. **Fuyi Xu:** Formal analysis. **Geng Tian:** Conceptualization; funding acquisition. **Yin Zhang:** Conceptualization; funding acquisition; writing – review and editing.

ACKNOWLEDGMENTS

We thank the technical supports from the technicians at biomedicine research center platform, Binzhou Medical University.

FUNDING INFORMATION

This research was funded by Taishan Scholar program (tsqn201812100, Z.Y.), Taishan Scholar program (20221145), the National Natural Science Foundation of China (No. 82103391, Y.Y.), Major Basic Research Project of Shandong Provincial Natural Science Foundation (ZR2019ZD27, T.G.), Special Project of Central Government for Local Science and Technology Development of Shandong Province (YDZX20203700001291, T.G.), Natural Science Foundation of Shandong Province (ZR2021MH292, Z.Y.), and Youth Science Foundation project of Shandong Province Natural Science Foundation (ZR2020QH242, Y.Y.).

CONFLICT OF INTEREST STATEMENT

All authors declare no conflict of interest. All authors have agreed to publish this manuscript.

ETHICS STATEMENT

Approval of the research protocol by an Institutional Reviewer Board: N/A.

Informed Consent: N/A.

Registry and the Registration No. of the study/trial: N/A.

Animal Studies: The study was conducted in accordance with the Declaration of Helsinki. Human paraffin-embedded tissue and the animal experiments in the present study were approved by the Ethics Committee of Binzhou Medical University (Yantai, China) (no. 2021-201, Mar 2021).

ORCID

Yang Yang  <https://orcid.org/0009-0004-4596-3609>

Chunhua Lin  <https://orcid.org/0000-0001-5225-3518>

REFERENCES

- Bray F, Ferlay J, Soerjomataram I, Siegel RL, Torre LA, Jemal A. Global cancer statistics 2018: GLOBOCAN estimates of incidence and mortality worldwide for 36 cancers in 185 countries. *CA Cancer J Clin*. 2018;68:394-424.
- Williamson SR, Taneja K, Cheng L. Renal cell carcinoma staging: pitfalls, challenges, and updates. *Histopathology*. 2019;74:18-30.
- Guida A, Sabbatini R, Gibellini L, De Biasi S, Cossarizza A, Porta C. Finding predictive factors for immunotherapy in metastatic renal-cell carcinoma: what are we looking for? *Cancer Treat Rev*. 2021;94:102157.
- Huang SY, Hou YG, Hu M, Hu JC, Liu XH. Clinical significance and oncogenic function of NR1H4 in clear cell renal cell carcinoma. *BMC Cancer*. 2022;22:995.
- Ducker GS, Rabinowitz JD. One-carbon metabolism in health and disease. *Cell Metab*. 2017;25:27-42.
- Moore LE, Hung R, Karami S, et al. Folate metabolism genes, vegetable intake and renal cancer risk in central Europe. *Int J Cancer*. 2008;122:1710-1715.
- Gibson TM, Brennan P, Han S, et al. Comprehensive evaluation of one-carbon metabolism pathway gene variants and renal cell cancer risk. *PLoS One*. 2011;6:e26165.
- Zhang L, Meng XX, Ju XB, et al. One-carbon metabolism pathway gene variants and risk of clear cell renal cell carcinoma in a Chinese population. *PLoS One*. 2013;8:e81129.
- Maddocks ODK, Athineos D, Cheung EC, et al. Modulating the therapeutic response of tumours to dietary serine and glycine starvation. *Nature*. 2017;544:372-376.
- Sullivan MR, Mattaini KR, Dennstedt EA, et al. Increased serine synthesis provides an advantage for tumors arising in tissues where serine levels are limiting. *Cell Metab*. 2019;29:1410-1421.e1414.
- Sanchez-Castillo A, Vooijs M, Kampen KR. Linking serine/glycine metabolism to radiotherapy resistance. *Cancers (Basel)*. 2021;13:1191.
- Tramonti A, Nardella C, di Salvo ML, Barile A, Cutruzzola F, Contestabile R. Human cytosolic and mitochondrial serine hydroxymethyltransferase isoforms in comparison: full kinetic characterization and substrate inhibition properties. *Biochemistry*. 2018;57:6984-6996.
- Xie M, Pei DS. Serine hydroxymethyltransferase 2: a novel target for human cancer therapy. *Invest New Drugs*. 2021;39:1671-1681.
- Wu X, Deng L, Tang D, et al. miR-615-5p prevents proliferation and migration through negatively regulating serine hydroxymethyltransferase 2 (SHMT2) in hepatocellular carcinoma. *Tumour Biol*. 2016;37:6813-6821.
- Bernhardt S, Bayerlova M, Vetter M, et al. Proteomic profiling of breast cancer metabolism identifies SHMT2 and ASCT2 as prognostic factors. *Breast Cancer Res*. 2017;19:112.
- Yang X, Wang Z, Li X, et al. SHMT2 desuccinylation by SIRT5 drives cancer cell proliferation. *Cancer Res*. 2018;78:372-386.
- Liu C, Wang L, Liu X, et al. Cytoplasmic SHMT2 drives the progression and metastasis of colorectal cancer by inhibiting beta-catenin degradation. *Theranostics*. 2021;11:2966-2986.
- Lee GY, Haverty PM, Li L, et al. Comparative oncogenomics identifies PSMB4 and SHMT2 as potential cancer driver genes. *Cancer Res*. 2014;74:3114-3126.
- Gupta R, Yang Q, Dogra SK, Wajapeyee N. Serine hydroxymethyltransferase 1 stimulates pro-oncogenic cytokine expression through sialic acid to promote ovarian cancer tumor growth and progression. *Oncogene*. 2017;36:4014-4024.

20. Paone A, Marani M, Fiascarelli A, et al. SHMT1 knockdown induces apoptosis in lung cancer cells by causing uracil misincorporation. *Cell Death Dis.* 2014;5:e1525.
21. Noh S, Kim DH, Jung WH, Koo JS. Expression levels of serine/glycine metabolism-related proteins in triple negative breast cancer tissues. *Tumour Biol.* 2014;35:4457-4468.
22. Dou C, Xu Q, Liu J, et al. SHMT1 inhibits the metastasis of HCC by repressing NOX1-mediated ROS production. *J Exp Clin Cancer Res.* 2019;38:70.
23. Huo FC, Xie M, Zhu ZM, Zheng JN, Pei DS. SHMT2 promotes the tumorigenesis of renal cell carcinoma by regulating the m6A modification of PPAT. *Genomics.* 2022;114:110424.
24. Wei Z, Song JL, Wang GH, et al. Deacetylation of serine hydroxymethyl-transferase 2 by SIRT3 promotes colorectal carcinogenesis. *Nat Commun.* 2018;9:4468.
25. Chesler EJ, Lu L, Shou S, et al. Complex trait analysis of gene expression uncovers polygenic and pleiotropic networks that modulate nervous system function. *Nat Genet.* 2005;37:233-242.
26. Mulligan MK, Mozhui K, Prins P, Williams RW. GeneNetwork: a toolbox for systems genetics. *Methods Mol Biol.* 2017;1488:75-120.
27. Lemonnier T, Dupre A, Jessus C. The G2-to-M transition from a phosphatase perspective: a new vision of the meiotic division. *Cell Div.* 2020;15:9.
28. Piano V, Alex A, Stege P, et al. CDC20 assists its catalytic incorporation in the mitotic checkpoint complex. *Science.* 2021;371:67-71.
29. Yam CQX, Lim HH, Surana U. DNA damage checkpoint execution and the rules of its disengagement. *Front Cell Dev Biol.* 2022;10:1020643.
30. Xu F, Gao J, Orgil BO, et al. Ace2 and Tmprss2 expressions are regulated by Dhx32 and influence the gastrointestinal symptoms caused by SARS-CoV-2. *J Pers Med.* 2021;11:1212.
31. Ashbrook DG, Arends D, Prins P, et al. A platform for experimental precision medicine: the extended BXD mouse family. *Cell Syst.* 2021;12:235-247.e239.
32. Ducker GS, Chen L, Morscher RJ, et al. Reversal of cytosolic one-carbon flux compensates for loss of the mitochondrial folate pathway. *Cell Metab.* 2016;23:1140-1153.
33. Lameirinhas A, Miranda-Goncalves V, Henrique R, Jeronimo C. The complex interplay between metabolic reprogramming and epigenetic alterations in renal cell carcinoma. *Genes (Basel).* 2019;10:264.
34. Pan S, Fan M, Liu Z, Li X, Wang H. Serine, glycine and onecarbon metabolism in cancer (review). *Int J Oncol.* 2021;58:158-170.
35. Li AM, Ye J. Reprogramming of serine, glycine and one-carbon metabolism in cancer. *Biochim Biophys Acta Mol Basis Dis.* 2020;1866:165841.
36. Gao X, Lee K, Reid MA, et al. Serine availability influences mitochondrial dynamics and function through lipid metabolism. *Cell Rep.* 2018;22:3507-3520.
37. Kottakis F, Nicolay BN, Roumane A, et al. Author correction: LKB1 loss links serine metabolism to DNA methylation and tumorigenesis. *Nature.* 2019;575:E5.
38. Monti M, Guiducci G, Paone A, et al. Modelling of SHMT1 riboregulation predicts dynamic changes of serine and glycine levels across cellular compartments. *Comput Struct Biotechnol J.* 2021;19:3034-3041.
39. Chang DZ, Ma Y, Ji B, et al. Increased CDC20 expression is associated with pancreatic ductal adenocarcinoma differentiation and progression. *J Hematol Oncol.* 2012;5:15.
40. Wang L, Zhang J, Wan L, Zhou X, Wang Z, Wei W. Targeting Cdc20 as a novel cancer therapeutic strategy. *Pharmacol Ther.* 2015;151:141-151.
41. Karra H, Repo H, Ahonen I, et al. Cdc20 and securin overexpression predict short-term breast cancer survival. *Br J Cancer.* 2014;110:2905-2913.
42. Taniguchi K, Momiyama N, Ueda M, et al. Targeting of CDC20 via small interfering RNA causes enhancement of the cytotoxicity of chemoradiation. *Anticancer Res.* 2008;28:1559-1563.
43. Giardina G, Brunotti P, Fiascarelli A, et al. How pyridoxal 5'-phosphate differentially regulates human cytosolic and mitochondrial serine hydroxymethyltransferase oligomeric state. *FEBS J.* 2015;282:1225-1241.

SUPPORTING INFORMATION

Additional supporting information can be found online in the Supporting Information section at the end of this article.

How to cite this article: Yang Y, Zhang M, Zhao Y, et al. HOXD8 suppresses renal cell carcinoma growth by upregulating SHMT1 expression. *Cancer Sci.* 2023;114:4583-4595. doi:[10.1111/cas.15982](https://doi.org/10.1111/cas.15982)